

## Raman Evidence for a Weakened O–O Bond in Mononuclear Low-Spin Iron(III)–Hydroperoxides

Raymond Y. N. Ho,<sup>†</sup> Gerard Roelfes,<sup>‡</sup> Ben L. Feringa,<sup>\*,‡</sup> and Lawrence Que, Jr.<sup>\*,†</sup>

Department of Chemistry and Center for Metals in Biocatalysis, University of Minnesota  
Minneapolis, Minnesota 55455

Department of Organic and Molecular Inorganic Chemistry  
Groningen Center for Catalysis and Synthesis  
University of Groningen, Nijenborgh 4, 9747 AG  
Groningen, The Netherlands

Received August 7, 1998

Iron–peroxo species have been proposed or demonstrated to be catalytic intermediates in the mechanisms of a number of mononuclear iron enzymes<sup>1,2</sup> and catalysts involved in alkane and arene hydroxylation and olefin epoxidation.<sup>3–5</sup> Among these is a subset that have low-spin iron(III) centers as indicated by rhombic EPR signals at  $g = 1.9–2.4$ . Four of these have been formulated to be [LFe–OOH] species based on electrospray ionization mass spectral (ESI-MS) data, where L = TPA,<sup>4,6</sup> N4Py,<sup>5</sup> Py5,<sup>7</sup> and the antitumor drug bleomycin<sup>8</sup> and are implicated in hydrocarbon oxidation reactions.<sup>3a–5,9,10</sup> Such low-spin iron(III)–hydroperoxo species are also likely to be involved in the chemistry of heme peroxidases, cytochrome P450, and related heme catalysts.<sup>2,11</sup> To date, no vibrational information has been obtained that provides insight into the relative bond strengths of the O–O and Fe–O bonds because of the short lifetimes of such complexes and their susceptibility to photodecomposition.<sup>3b,5</sup> By excitation into the peroxide-to-iron(III) charge-transfer band at much lower energy, we have obtained resonance Raman spectra of [Fe(III)(TPA)(OOH)]<sup>2+</sup> (**1**) and [Fe(III)(N4Py)(OOH)]<sup>2+</sup> (**2**) which shed light into the reactivity of these species.

Previously, we have reported that the addition of excess H<sub>2</sub>O<sub>2</sub> to [Fe(II)(TPA)(CH<sub>3</sub>CN)<sub>2</sub>]<sup>2+</sup> or [Fe(II)(N4Py)(CH<sub>3</sub>CN)<sub>2</sub>]<sup>2+</sup> at low temperatures gives rise to purple low-spin Fe(III)–OOH intermediates, **1** and **2**, with  $\lambda_{\text{max}}$ 's at 538 nm<sup>4</sup> ( $\epsilon \approx 1000 \text{ M}^{-1} \text{ cm}^{-1}$ ) or 532 nm<sup>5</sup> ( $\epsilon \approx 1100 \text{ M}^{-1} \text{ cm}^{-1}$ ), respectively. The Raman spectrum of **1** (Figure 1A), obtained by excitation into the long wavelength tail of its peroxo-to-iron(III) charge-transfer band, shows two resonance-enhanced features at 626 and 789 cm<sup>-1</sup>,

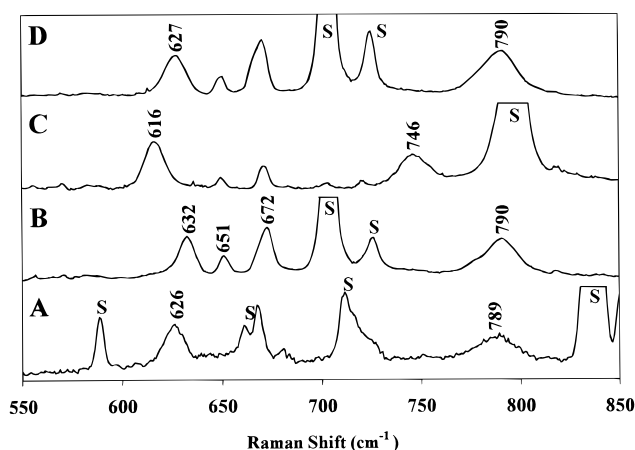


**Figure 1.** Resonance Raman spectra of **1** and **2**. A. 50 mM H<sub>2</sub>O<sub>2</sub> dissolved in CD<sub>3</sub>CN was added to 10 mM [Fe(II)(TPA)(CH<sub>3</sub>CN)<sub>2</sub>]<sup>2+</sup> in 4/1 CD<sub>3</sub>CN/THF at –50 °C. The spectrum was obtained with 568.2 nm laser excitation at 20 mW power at the sample. B. 50 mM H<sub>2</sub>O<sub>2</sub> was added to 10 mM [Fe(II)(N4Py)(CH<sub>3</sub>CN)<sub>2</sub>]<sup>2+</sup> in *d*<sub>6</sub>-acetone at –10 °C. The spectrum was obtained with 615 nm laser excitation at 20 mW power at the sample. C. Same as B, except H<sub>2</sub><sup>18</sup>O<sub>2</sub> and acetone were used. D. Same as B, except H<sub>2</sub>O<sub>2</sub> diluted in D<sub>2</sub>O was used.

while that of **2** (Figure 1B) shows four features at 632, 651, 672, and 790 cm<sup>-1</sup>. Excitation profile studies confirm that these vibrations are all associated with the peroxo-to-iron(III) charge-transfer transition. Due to experimental complications,<sup>12</sup> isotope data could only be obtained for **2**. With H<sub>2</sub><sup>18</sup>O<sub>2</sub> (Figure 1C), only the features at 632 and 790 cm<sup>-1</sup> of **2** downshift by 16 and 44 cm<sup>-1</sup>, respectively, while the 651 and 672 cm<sup>-1</sup> features are unaffected.<sup>13</sup> The vibrations around 630 and 790 cm<sup>-1</sup> are thus associated with the Fe–OOH moiety.

Resonance Raman spectra of iron–peroxide complexes typically exhibit two resonance enhanced features, a  $\nu(\text{O}–\text{O})$  between 800 and 900 cm<sup>-1</sup> and a  $\nu(\text{M}–\text{O})$  between 400 and 503 cm<sup>-1</sup> (Table 1). The 790 cm<sup>-1</sup> feature in **1** and **2** is best assigned as the  $\nu(\text{O}–\text{O})$ . This assignment is strongly justified by the –44 cm<sup>-1</sup> shift for this feature upon <sup>18</sup>O substitution in **2** (Figure 1C), which matches well the shift of –45 cm<sup>-1</sup> predicted by Hooke's law for a diatomic O–O stretch. As shown in Table 1, 790 cm<sup>-1</sup> is the lowest  $\nu(\text{O}–\text{O})$  of any iron–peroxo species, including the two characterized  $\eta^2$ -peroxo–iron species. This comparison suggests that the O–O bond is significantly weakened in **1** and **2**.

The assignment of the 632 cm<sup>-1</sup> feature is less certain. While it is initially tempting to assign it to a  $\nu(\text{Fe}–\text{O})$ , Fe–O vibrations for other iron–peroxo species are significantly lower in energy and are typically observed between 400 and 503 cm<sup>-1</sup> (Table 1). Furthermore the use of H<sub>2</sub><sup>18</sup>O<sub>2</sub> affords a shift of only –16 cm<sup>-1</sup>, which is about half that predicted by Hooke's law calculations for a pure Fe–O vibration (–28 cm<sup>-1</sup>). Calculations for an Fe–OO vibration (–23 cm<sup>-1</sup>) or an Fe–OOH vibration (–22 cm<sup>-1</sup>) afford shifts that approach the observed value, but it is clear that this vibration must involve the coupling of a number of modes. Similar complications have been noted in the analysis of Raman

(12) H<sub>2</sub><sup>18</sup>O<sub>2</sub> is commercially available only as a 2% aqueous solution. Such a solution freezes rapidly when introduced to a 9/1 CH<sub>3</sub>CN/THF at –40 to –50 °C and prevents the generation of **1** for Raman studies. With H<sub>2</sub><sup>16</sup>O<sub>2</sub>, this problem can be avoided by diluting the aqueous 30% H<sub>2</sub>O<sub>2</sub> with CH<sub>3</sub>CN.

(13) Scrutiny of the spectra in Figure 1 may indicate a downshift for the 672 cm<sup>-1</sup> feature. However this is only an apparent shift, as the solvent *d*<sub>6</sub>-acetone has a weak feature at 668 cm<sup>-1</sup> which overlaps with the 672 cm<sup>-1</sup> feature in **2**. Curve fits of the Raman spectra gave 651 and 672 cm<sup>-1</sup> for <sup>16</sup>O, 650 and 671 cm<sup>-1</sup> for <sup>18</sup>O, and 650 and 671 cm<sup>-1</sup> for <sup>2</sup>H. The 1 cm<sup>-1</sup> downshifts observed are within the uncertainty of our instrument.

<sup>†</sup> University of Minnesota.

<sup>‡</sup> University of Groningen.

(1) Que, L., Jr.; Ho, R. Y. N. *Chem. Rev.* **1996**, *96*, 2607–2624.

(2) Sono, M.; Roach, M. P.; Coulter, E. D.; Dawson, J. H. *Chem. Rev.* **1996**, *96*, 2841–2887.

(3) (a) Hecht, S. M. *Acc. Chem. Res.* **1986**, *19*, 383–391. (b) Guajardo, R. J.; Hudson, S. E.; Brown, S. J.; Mascharak, P. K. *J. Am. Chem. Soc.* **1993**, *115*, 7971–7977. (c) Nam, W.; Ho, R.; Valentine, J. S. *J. Am. Chem. Soc.* **1991**, *113*, 7052–7054.

(4) Kim, C.; Chen, K.; Kim, J.; Que, L., Jr. *J. Am. Chem. Soc.* **1997**, *119*, 5964–5965.

(5) Lubben, M.; Meetsma, A.; Wilkinson, E. C.; Feringa, B.; Que, L., Jr. *Angew. Chem., Int. Ed. Engl.* **1995**, *34*, 1512–1514.

(6) Abbreviations used: BLM = bleomycin, DFT = density functional theory, EDTA = ethylenediaminetetraacetic acid, N4Py = *N*-(bis(2-pyridyl)-methyl)-*N,N*-bis(2-pyridylmethyl)amine, OEP = 2,3,7,8,12,13,17,18-octaethyl-21H,23H-porphine, Py5 = 2,6-bis-(bis(2-pyridyl)methoxymethane)pyridine, T(2-*N*-Me)PyP = tetrakis(2-*N*-methylpyridiniumyl)-porphyrinato, TPA = tris-(2-pyridylmethyl)amine.

(7) de Vries, M. E.; La Crois, R. M.; Roelfes, G.; Kooijman, H.; Spek, A. L.; Hage, R.; Feringa, B. L. *J. Chem. Soc., Chem. Commun.* **1997**, 1549–1550.

(8) Sam, J. W.; Tang, X.-J.; Peisach, J. *J. Am. Chem. Soc.* **1994**, *116*, 6, 5250–5256.

(9) Stubbe, J.; Kozarich, J. W. *Chem. Rev.* **1987**, *87*, 1107–1136.

(10) Kane, S. A.; Hecht, S. M. *Prog. Nucleic Acid Res. Mol. Biol.* **1994**, *49*, 313–352.

(11) *Cytochrome P-450. Structure, Mechanism and Biochemistry*; Ortiz de Montellano, P. R., Ed.; Plenum Press: New York, 1986.

**Table 1.** Reported Resonance Raman Features of Iron–Peroxide Complexes

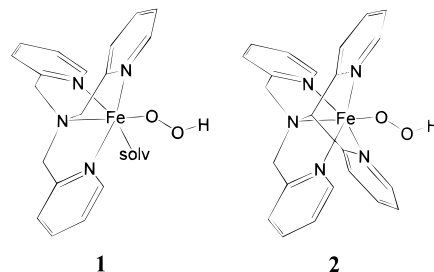
complex	$\nu_{\text{Fe-L}}$ ( $\text{cm}^{-1}$ ) <sup>a</sup>	$\nu_{\text{O-O}}$ ( $\text{cm}^{-1}$ )	ref
[Fe(TPA)(OOH)] <sup>2+</sup>	626 <sup>b</sup>	789	this work
[Fe(N4Py)(OOH)] <sup>2+</sup>	632 <sup>b</sup>	790	this work
[Fe(OEP)( $\eta^2$ -O <sub>2</sub> )] <sup>-</sup>	n.o.	805	14
[Fe(III)(EDTAH)( $\eta^2$ -O <sub>2</sub> )] <sup>2-</sup>	n.o.	815	15
oxyhemerythrin [Fe( $\eta^1$ -OOH)]	503	844	16,17
Fe <sub>2</sub> ( $\mu$ -1,2-O <sub>2</sub> ) species	415–476	848–900	18

<sup>a</sup> L = O or OOH. <sup>b</sup> Observed feature for the coupled Fe–OOH mode.

data for the related [Fe(TPA)(OO'Bu)]<sup>2+</sup> species.<sup>19</sup> The 632  $\text{cm}^{-1}$  feature also exhibits a 5  $\text{cm}^{-1}$  downshift with <sup>2</sup>H<sub>2</sub>O<sub>2</sub> (Figure 1D) compared to a calculated shift of –6  $\text{cm}^{-1}$  for a  $\nu(\text{Fe}–\text{OOH})$ . This <sup>2</sup>H isotope shift strongly supports the presence of a hydroperoxide ligand initially deduced from ESI-MS data.<sup>5</sup> The sensitivity of the 632  $\text{cm}^{-1}$  feature to both <sup>18</sup>O and <sup>2</sup>H from H<sub>2</sub>O<sub>2</sub> indicates a coupled mode that arises from an Fe–OOH unit.

In contrast to the high spin centers of other characterized iron–peroxo species in Table 1, the iron(III) centers in **1** and **2** are low-spin. This change in the spin state causes a decrease in the ionic radius which may result in the strengthening of the Fe–O bond. The pentadentate N4Py ligand may also promote a stronger Fe–O bond as demonstrated by the very short (1.79 Å) Fe–OMe bond in [Fe(III)(N4Py)(OMe)]<sup>2+</sup><sup>20</sup> which is also found in the closely related [Fe(III)(Py5)(OMe)]<sup>2+</sup>.<sup>21</sup> These factors may contribute to the unusually high energy observed for the vibration of the Fe–OOH mode.

The Raman features around 630 and 790  $\text{cm}^{-1}$  clearly distinguish **1** and **2** from other metal–peroxide species (Table 1) and may represent the Raman signature for mononuclear low-

**Figure 2.** Proposed binding mode of the hydroperoxide in **1** and **2**.

spin Fe(III)–OOH species. Given the fact that the few structurally characterized M–OOH complexes all have  $\eta^1$  (end-on) binding modes,<sup>22,23</sup> it is likely that the hydroperoxides in **1** and **2** are similarly bound (Figure 2). The observation that these low-spin Fe(III)–OOH species have a  $\nu(\text{O}–\text{O})$  at least 50  $\text{cm}^{-1}$  lower than that of the high-spin peroxo complexes suggests that the low-spin center may weaken the O–O bond. This notion is supported by recent nonlocal DFT calculations on the putative Fe–OOH species in cytochrome P450.<sup>24</sup> This weakened bond would then be primed for O–O bond cleavage to convert the low-spin iron(III) ( $t_{2g}^5$ ) center with minimal electronic reorganization to low-spin iron(IV) ( $t_{2g}^4$ )–oxo or iron(V) ( $t_{2g}^3$ )–oxo species, which are generally accepted as the key oxidants in the mechanisms of many heme-catalyzed oxidations.<sup>2,11</sup> Indeed **1** and **2** are the only peroxo species in Table 1 associated with the catalytic oxidation of relatively inert hydrocarbons such as cyclohexane.<sup>4,5</sup> Similar arguments may be applied to rationalize the involvement of low-spin Fe(III)–OOH species in the catalytic cycles of bleomycin<sup>3a,9,10</sup> and several heme enzymes.<sup>2,11</sup> Our Raman data thus shed light into one mechanism by which dioxygen can be activated at mononuclear iron sites, illustrating a common thread that underlies iron metallobiochemistry in both heme and non-heme systems.

**Acknowledgment.** This work was supported by the National Institutes of Health (GM-33162) and Unilever Research Laboratory, Vlaardingen (The Netherlands). R.Y.N.H. acknowledges a National Institutes of Health postdoctoral fellowship (GM-17849).

JA982812P

(21) Jonas, R. T.; Stack, T. D. P. *J. Am. Chem. Soc.* **1997**, *119*, 8566–8567.

(22) Holmes, M. A.; Le Trong, I.; Turley, S.; Sieker, L. C.; Stenkamp, R. E. *J. Mol. Biol.* **1991**, *218*, 583–593.

(23) (a) Le Carpentier, J. M.; Mitschler, A.; Weiss, R. *Acta Crystallogr., Sect. B* **1972**, *1288*–1298. (b) Carmona, D.; Lamata, M. P.; Ferrer, J.; Modrego, J.; Perales, M.; Lahoz, F. J.; Atencio, R.; Oro, L. A. *J. Chem. Soc., Chem Commun.* **1994**, 575–576. (c) Wada, A.; Harata, M.; Hasegawa, K.; Jitsukawa, K.; Masuda, H.; Mukai, M.; Kitagawa, T.; Einaga, H. *Angew. Chem., Int. Ed.* **1998**, *37*, 798–799.

(24) Harris, D. L.; Loew, G. H. *J. Am. Chem. Soc.* **1998**, *120*, 8941–8948.

(14) McCandlish, E.; Miksztal, A. R.; Nappa, M.; Sprenger, A. Q.; Valentine, J. S.; Stong, J. D.; Spiro, T. G. *J. Am. Chem. Soc.* **1980**, *102*, 4268–4271.

(15) Ahmad, S.; McCallum, J. D.; Shiemke, A. K.; Appelman, E. H.; Loehr, T. M.; Sanders-Loehr, J. *Inorg. Chem.* **1988**, *27*, 2230–2233.

(16) Kurtz, D. M., Jr.; Shriver, D. F.; Klotz, I. M. *J. Am. Chem. Soc.* **1976**, *98*, 5033.

(17) Shiemke, A. K.; Loehr, T. M.; Sanders-Loehr, J. *J. Am. Chem. Soc.* **1984**, *106*, 4951–4956.

(18) (a) Murch, B. P.; Bradley, F. C.; Que, L., Jr. *J. Am. Chem. Soc.* **1986**, *108*, 5027–5028; (b) Kitajima, N.; Fukui, H.; Moro-oka, Y.; Mizutani, Y.; Kitagawa, T. *J. Am. Chem. Soc.* **1990**, *112*, 6402–6403. (c) Brennan, B. A.; Chen, Q.; Juarez-Garcia, C.; True, A. E.; O'Connor, C. J.; Que, L., Jr. *Inorg. Chem.* **1991**, *30*, 1937–1943. (d) Kitajima, N.; Tamura, N.; Tanaka, M.; Moro-oka, Y. *Inorg. Chem.* **1992**, *31*, 3342–3343. (e) Dong, Y.; Ménage, S.; Brennan, B. A.; Elgren, T. E.; Jang, H. G.; Pearce, L. L.; Que, L., Jr. *J. Am. Chem. Soc.* **1993**, *115*, 1851–1859. (f) Kim, K.; Lippard, S. J. *J. Am. Chem. Soc.* **1996**, *118*, 4914–4915. (g) Dong, Y.; Zang, Y.; Kauffmann, K.; Shu, L.; Wilkinson, E. C.; Münck, E.; Que, L., Jr. *J. Am. Chem. Soc.* **1997**, *119*, 12683–12684.

(19) Zang, Y.; Kim, J.; Dong, Y.; Wilkinson, E. C.; Appelman, E. H.; Que, L., Jr. *J. Am. Chem. Soc.* **1997**, *119*, 4197–4205.

(20) Roelfes, G.; Chen, K.; Que, L., Jr.; Feringa, B. L., unpublished results.